Structure of the ZU5-ZU5-UPA-DD tandem of ankyrin-B reveals interaction surfaces necessary for ankyrin function

Chao Wang[a], Cong Yu[a], Fei Ye[a], Zhiyi Wei[a,b,1], and Mingjie Zhang[a,1]

[a]Division of Life Science, State Key Laboratory of Molecular Neuroscience, Hong Kong University of Science and Technology, Clear Water Bay, Kowloon, Hong Kong; and [b]Institute for Advanced Study, Hong Kong University of Science and Technology, Clear Water Bay, Kowloon, Hong Kong

Edited by Vann Bennett, Duke University Medical Center, Durham, NC, and approved January 31, 2012 (received for review January 13, 2012)

Ankyrin-R/B/G (encoded by *ANK1/2/3*, respectively) are a family of very large scaffold proteins capable of anchoring numerous receptors and ion channels to specific, spectrin-containing membrane micro-domains. Hereditary mutations of ankyrins are known to be associated with diseases including spherocytosis, cardiac arrhythmia, and bipolar disorder in humans, although the underlying molecular bases are poorly understood. The middle spectrin-binding domain of ankyrins contains highly conserved ZU5-ZU5-UPA-DD domains arranged into the ZZUD tandem. Curiously, most of the disease-causing mutations in the tandem have no apparent impact on the spectrin binding of ankyrins. The high resolution structure of the ankyrin-B ZZUD tandem determined here reveals that the ZU5-ZU5-UPA domains form a tightly packed structural supramodule, whereas DD is freely accessible. Although the formation of the ZZU supramodule does not influence the spectrin binding of ankyrins, mutations altering the interdomain interfaces of ZZU impair the functions of ankyrin-B&G. Our structural analysis further indicates that the ZZU supramodule of ankyrins has two additional surfaces that may bind to targets other than spectrin. Finally, the structure of the ankyrin ZZUD provides mechanistic explanations to many disease-causing mutations identified in ankyrin-B&R.

ankyrin-B syndrome | cytoskeleton | PIDD | UNC5

Ankyrins are a family of adaptor proteins required for the construction and maintenance of specialized membrane domains in various tissues via anchoring specific membrane proteins to spectrin-based cytoskeletons (see refs. 1 and 2 for reviews). Vertebrates contain three ankyrins: ankyrin-R, -B, and -G, all containing an N-terminal membrane-binding domain (MBD), a central spectrin-binding domain (SBD), a death domain (DD) with ill-defined functions, and a variable C-terminal regulatory domain (2) (Fig. 1*C*). Ankyrin-R, the first identified ankyrin from erythrocytes, is also expressed in other tissues (3, 4). Ankyrin-B, originally identified in brain, functions in many tissues including in the cardiac and skeletal muscles (2). Ankyrin-G, the most broadly expressed ankyrin, is critical for the formation and stabilization of axon initial segments of neurons, the biogenesis of lateral membrane domains of epithelia as well as other tissue functions (2, 5–8). Loss-of-function mutations in ankyrins are associated with hereditary diseases in humans. For example, a number of loss-of-function mutations of ankyrin-R are known to cause hereditary spherocytosis (9). Genetic variants of ankyrin-G are associated with bipolar disorder (10–14). Many missense mutations of ankyrin-B have been linked to inherited cardiac arrhythmia known as the "ankyrin-B syndrome" (15). Curiously, although MBD is responsible for binding to most of known ankyrin-association proteins, most of the ankyrin-B syndrome mutations are located in the SBD, DD, and regulatory domains, and these mutations do not seem to affect the binding of ankyrins to spectrin (16). These findings suggest that SBD is involved in functions other than binding to spectrin, although very little is known in this regard.

Ankyrin SBD consists of three highly conserved domains, two ZU5 and a UPA domains arranged into a ZU5-ZU5-UPA (termed as ZZU) tandem (17). The high conservation nature of SBD in all ankyrins (across isoforms and species) strongly indicates that SBD plays critical roles in ankyrin's functions. The best-documented function of SBD is to bind to spectrin (β-spectrin specifically), which requires the first ZU5 domain ($ZU5^N$) only (16, 18). Thus, the second ZU5 domain ($ZU5^C$) and the UPA domain of ankyrins are likely to be involved in functions other than binding to spectrin. Supporting this notion, a recent study of ankyrin-B and -G showed that a number of mutations in $ZU5^C$ and UPA had no impact on their binding to spectrin but led to functional impairment of ankyrins (8).

Our recent study of the ZU5-UPA-DD tandem of netrin receptor UNC5b revealed that its ZU5 interacts with both UPA and DD to form a supramodule with an auto-inhibited conformation (17). Because the ankyrin ZZU tandem is also followed by a DD, we proposed that $ZU5^C$, UPA, and DD of ankyrins may also form a similar auto-inhibited conformation. PIDD, a scaffold protein that acts as a molecular switch in controlling programmed cell death (19), contains a similar ZZUD tandem (Fig. 1*C*). It remains to be established why ankyrins and PIDD contain two ZU5 domains arranged next to each other.

Here, we determined the high resolution crystal structure of the ZU5-ZU5-UPA-DD tandem (termed as ZZUD) of ankyrin-B, which reveals that the ZZU tandem indeed forms a structural supramodule. Within the supramodule, $ZU5^N$ but not $ZU5^C$ interacts with UPA. The $ZU5^N$/UPA and the $ZU5^N$/$ZU5^C$ interactions do not interfere ankyrin's binding to spectrin. Further structural analysis of the ZZU tandem suggests that it contains two additional target binding sites, which may allow ankyrins to bind target proteins other than spectrin. Unexpectedly, unlike in UNC5b, DD in ankyrin-B ZZUD is not sequestered by the ZZU tandem. The structure of the ankyrin-B ZZUD tandem provides mechanistic explanations to a number of disease-causing mutations of ankyrins.

Results and Discussion

The Overall Structure of Ankyrin-B ZZUD. To understand how the $ZU5^N$, $ZU5^C$, UPA, and DD domains of ankyrins assemble together to perform their functions, we attempted to solve the structure of ankyrin-B ZZUD by X-ray crystallography. After extensive trials, we discovered that the deletion of a nine-residue

Author contributions: C.W., C.Y., Z.W., and M.Z. designed research; C.W., C.Y., F.Y., and Z.W. performed research; C.W., C.Y., F.Y., Z.W., and M.Z. analyzed data; and Z.W. and M.Z. wrote the paper.

The authors declare no conflict of interest.

This article is a PNAS Direct Submission.

Data deposition: The atomic coordinates and structure factors have been deposited in the Protein Data Bank, www.pbd.org (PDB ID code 4D8O).

[1]To whom correspondence may be addressed. E-mail: zwei@ust.hk or mzhang@ust.hk.

This article contains supporting information online at www.pnas.org/lookup/suppl/doi:10.1073/pnas.1200613109/-/DCSupplemental.

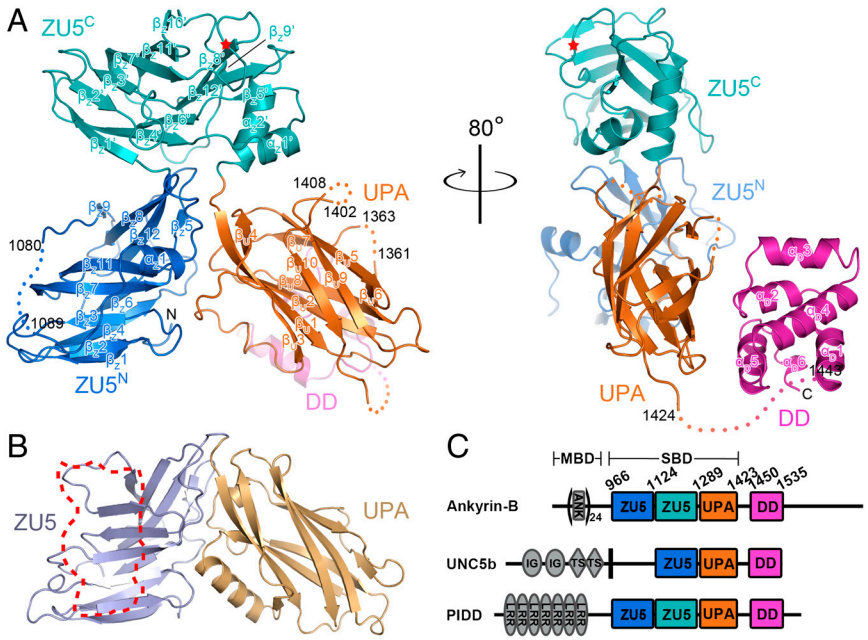

Fig. 1. Overall structure of ankyrin-B ZZUD. (*A*) Ribbons diagram representation of the crystal structure of ankyrin-B ZZUD with $ZU5^N$ (blue), $ZU5^C$ (cyan), UPA (orange), and DD (purple) drawn in their specific colors. The same color code is used throughout the rest of the figures. The disordered regions are indicated by dotted lines with starting and end residues number labeled. The nine-residue deletion site is indicated by a red star. (*B*) Comparing with ankyrin-B, the ZU5 and UPA domains of UNC5b interact with each other following a similar manner. The DD binding region in ZU5 of UNC5b is highlighted with a dotted trace. (*C*) Domain architectures of the ZU5-UPA-DD containing proteins in the eukaryotes genomes. The domain boundaries of ankyrin-B ZZUD are defined based on the structure determined in this work.

fragment in a solvent-exposed loop of $ZU5^C$ (Figs. 1*A* and 2) enabled us to obtain high diffraction-quality crystals of ZZUD. The ankyrin-B ZZUD structure was determined at a 2.2-Å resolution by molecular replacement (Table S1). The final structural model contains most of residues from ankyrin-B ZZUD except for a few flexible loops (Fig. 1*A*).

The four domains in the ankyrin-B ZZUD structure are well-defined (Fig. 1*A*). Despite of a lower than 20% amino acid sequence identity, the two ZU5 domains share a similar overall fold with an rmsd of approximately 2 Å among approximately 110 aligned residues. Each ZU5 domain contains approximately 150 residues and folds into a β-strand rich structure with two antiparallel sheets interacting with each other in parallel to form a β-sandwich. One obvious difference between the two ZU5 domains is that $ZU5^C$ contains an additional C-terminal α-helix (α_Z2'), which covers the hydrophobic surface of the β-sheet and presumably stabilizes the domain (Fig. 1*A*). UPA also contains two antiparallel β-sheets but with a distinct topology from those of ZU5. Extensive interactions between the two ZU5 domains and between $ZU5^N$ and UPA domain stabilize the overall structure of the ZZU tandem, which adopts a cloverleaf-like architecture (Fig. 1*A*, *Left*). We note that $ZU5^N$ and UPA interact with each other mainly through their loop regions (Fig. 1*A*), and such ZU5/UPA interaction mode has also been observed in UNC5b (17) (Fig. 1*B*). Although being right next to each other in their primary sequences, $ZU5^C$ makes few contacts with UPA (Fig. 1*A*). The two ZU5 domains are separated by only one residue, and $ZU5^C$ and UPA are connected by a three-residue loop. Such short interdomain linkers also physically restrain the mobility of these three domains. Ankyrin-B DD adopts a typical death domain fold consisting of six helices, which is essentially identical to the solution structure of the isolated ankyrin-B DD with an rmsd value <1.0 Å. In contrast to the extensive interactions between $ZU5^N$ and $ZU5^C$ and between $ZU5^N$ and UPA that lead to the formation of a stable ZZU supramodule, DD only loosely interacts with UPA (Fig. 1*A*; see below for details).

The ZZU Tandem Forms a Structural Supramodule. The ZZU structure of ankyrin-B is mainly stabilized by the interactions of $ZU5^N$ with $ZU5^C$ and UPA, respectively. The buried surface areas of the $ZU5^N$/UPA and $ZU5^N$/$ZU5^C$ interfaces are approximately 1,600 $Å^2$ and approximately 1,200 $Å^2$, respectively. The residues forming the two interfaces are highly conserved among all ankyrins (Fig. 2), indicating that the $ZU5^N$/UPA and $ZU5^N$/$ZU5^C$ interactions and the overall architecture of the ZZU tandem observed in ankyrin-B are shared by other ankyrins as well.

The $ZU5^N$/UPA interface is primarily formed by residues from the loops of the two domains as well as two residues from β1 (Y1293) and β4 (E1341) of UPA (Fig. 3*A*). Three pairs of charge–charge interactions, formed by $R1055_{ZU5N}$ and $E1341_{UPA}$, $R1105_{ZU5C}$ and $D1339_{UPA}$, $R1029_{ZU5N}$ and $D1319_{UPA}$/$D1322_{UPA}$, are situated across the entire interface and thus are likely to be critical for the interdomain stability (Fig. 3*A*). Of the three pairs of the charged interactions, the $R1029_{ZU5N}$/$D1319_{UPA}$ pair is buried in the interface and is likely to be particularly important for the $ZU5^N$/UPA interaction. The $ZU5^N$/UPA interface is further stabilized by several hydrogen bonds as well as hydrophobic interactions (Fig. 3*A*).

The $ZU5^N$/$ZU5^C$ interface consists of residues from the β4/β5 loop, the β7/β8-loop, and β12 of $ZU5^N$ and β1′, β4′, the β4′/α1′-loop, and α2′ of $ZU5^C$ (Fig. 3*B*). These residues bridge the two domains together through both sidechain–sidechain and sidechain–main-chain hydrogen bonds (Fig. 3*B*). Compared with the $ZU5^N$/UPA interface, the $ZU5^N$/$ZU5^C$ interface contains much less residues and thus may be less rigid. However, because the two ZU5 domains are linked by only one residue, the degree of inter-ZU5 flexibility is limited.

We note with interest that the isolated $ZU5^N$ is well-folded (20), whereas the isolated $ZU5^C$ and UPA were always expressed as inclusion bodies, suggesting that $ZU5^C$ and UPA are not properly folded when expressed individually and may be stabilized in the ZZU supramodule via the interactions with $ZU5^N$. Together, our structure strongly indicates that the ZZU tandem forms an integral structural supramodule, which is likely to be required for ankyrin's functions.

The Intramolecular Interactions in the ZZU Tandem Do Not Affect the β-Spectrin Binding of $ZU5^N$. Ankyrin SBD interacts with β-spectrin via its $ZU5^N$ (16, 18, 20). Because $ZU5^N$ interacts with both UPA and $ZU5^C$, one must wonder whether such intramolecular interactions might have any impact on the ankyrin/spectrin interaction. To answer this question, we built an ankyrin-B ZZUD/β-spectrin repeats 13–15 (R13-15) complex structure model by superimposing the $ZU5^N$ structure of ankyrin-B ZZUD with that of the ankyrin-R $ZU5^N$/spectrin R13-15 complex (18) (Fig. 4). It is clear from the model that $ZU5^C$ is far away from the $ZU5^N$/β-spectrin

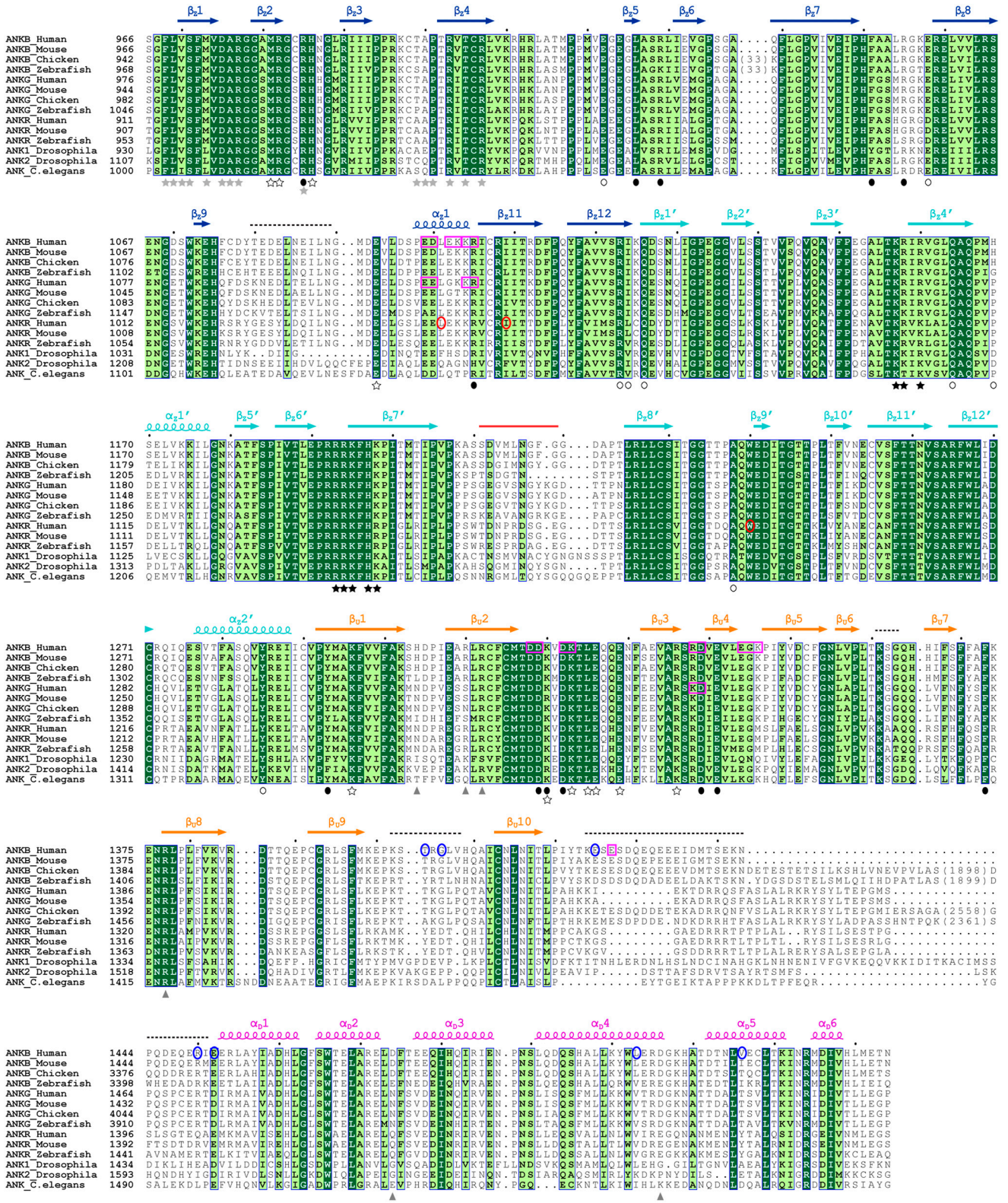

Fig. 2. Sequence alignment of the ZZUD tandems from the ankyrin family members. In this alignment, residues that are absolutely conserved and highly conserved are highlighted in dark and light green, respectively. The secondary structural elements are indicated above the alignment and the coloring scheme matches with the structure of the protein shown in Fig. 1*A*. The nine deleted residues in the crystal structure are marked by a red line. The disordered regions (Fig. 1*A*) are indicated by dashed lines. The amino acid residues involved in the formation of the $ZU5^N$/UPA and $ZU5^N$/$ZU5^C$ interfaces are indicated with solid and open circles, respectively. The residues involved in the UPA/DD interaction are indicated by gray triangles. The residues involved in formation of the conserved surface across $ZU5^N$ and UPA and formation of the highly conserved, positively charged surface of $ZU5^C$ are indicated by hollow and solid stars, respectively. The residues involved in spectrin binding are indicated by gray stars. The identified loss-of-function mutations in ankyrin-B and -G (8, 21) are highlighted by pink open boxes. These mutations do not affect the spectrin binding of the ankyrins. The mutations of amino acids that cause ankyrin-B syndrome and hereditary spherocytosis are labeled with blue and red circles, respectively.

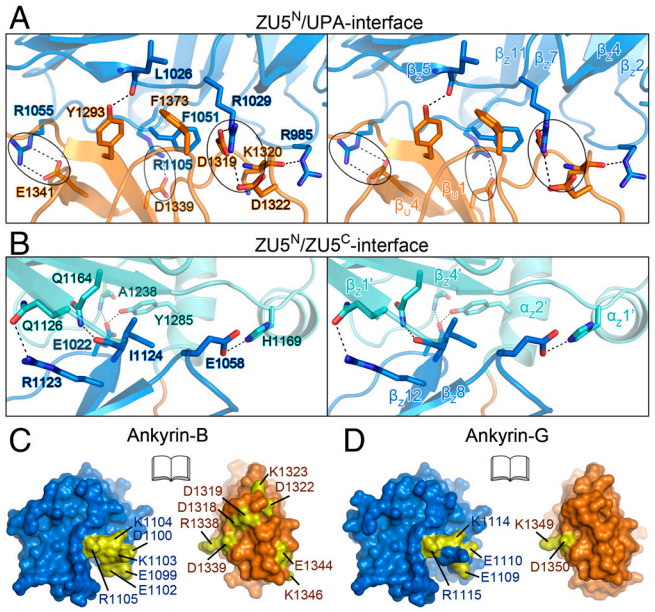

Fig. 3. The ZU5^N/UPA and ZU5^N/ZU5^C interfaces of ankyrin-B ZZUD. The molecular details are shown for the ZU5^N/UPA (*A*) and ZU5^N/ZU5^C (*B*) interfaces. The salt bridges and hydrogen bonds are indicated as dashed lines. The three charge pairs in the ZU5^N/UPA interface are highlighted by circles. The open-book views of the surfaces of the ZU5^N/UPA interfaces in ankyrin-B (*C*) and -G (*D*) demonstrate that the identified loss-of-function mutations (colored in yellow) in ankyrin-B and -G (8, 21) are concentrated within or in the vicinity of the ZU5^N/UPA interfaces of both ankyrins. The ankyrin-G ZZU structures are modeled by using the ankyrin-B ZZU structure as the template.

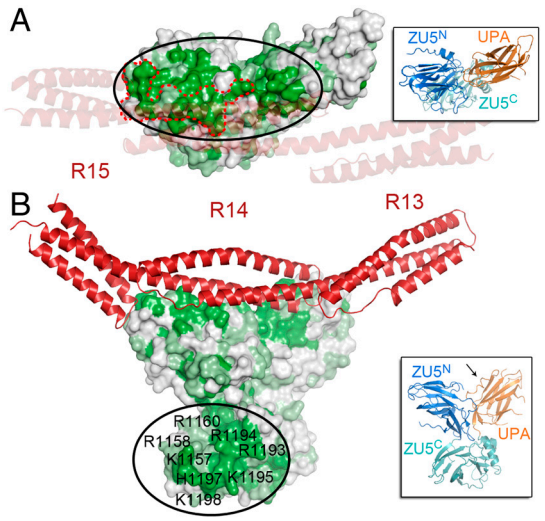

Fig. 4. The ZZU tandem in ankyrins contains two highly conserved potential target protein-interacting surfaces. The structure of the ankyrin-B ZZU/β-spectrin R13-15 complex was modeled by superimposing ZU5^N in the ankyrin-B ZZUD structure and that in the ankyrin-R ZU5^N/β-spectrin R13-15 complex structure and showed with the top view (*A*) and the lateral view (*B*). In this modeled complex structure, the ZZU tandem is drawn in surface representation. Surface residues that are absolutely conserved, highly conserved, and not conserved according to the sequence alignment in Fig. 2, are colored in green, light green, and white, respectively. The two large conserved regions on the ZZU tandem are highlighted by circles. In *A*, the spectrin-binding surface on ZU5^N is highlighted by a red dot trace; and for displaying the covered surface of the ZZU tandem, the β-spectrin R13-15 structure is shown as transparent ribbons. The highly conserved and positively charged surface residues of ZU5^C are labeled. The insets show the orientations of the ankyrin-B ZZUD in the complex structure model in *A* and *B*, respectively. The β2/β3-loop of UPA is indicated by an arrow.

interface, thus is not expected to have any impact on the complex formation. Although UPA is physically close to β-spectrin R13-14, the contact between UPA and β-spectrin is minimal (Fig. 4). Thus, it is predicted that UPA is unlikely to have appreciable impact on the ZU5^N/β-spectrin interaction either. Fully consistent with the above structure-based prediction, the K_d values of the ZZUD/β-spectrin and ZZUD_ΔUPA/β-spectrin complexes are essentially identical (Table S2). In addition, mutations of residues in the interdomain interfaces that are expected to disrupt the ZU5^N/UPA and ZU5^N/ZU5^C interactions do not affect the ZU5^N/spectrin interaction either (Table S2). Together, our biochemical and structural analysis demonstrates that the formation of the ZZU supramodule does not affect the spectrin binding of ZU5^N. Our finding is fully consistent with the previously reported observations showing that ZU5^N is necessary and sufficient for ankyrins to bind to spectrin (16, 18, 20).

The ZU5^N/UPA Interaction Is Required for Ankyrins' Function Other than Binding to Spectrin. Although ZU5^N is necessary and sufficient for binding to spectrin, the extremely high amino acid sequence conservation of the entire ZZU tandem among ankyrins throughout evolution argues for indispensable functional roles of their ZU5^C and UPA domains. Recently, Kizhatil et al. used an alanine-scanning-based approach and identified a number of residues within the ZZU tandems that are functionally important for ankyrin-B and -G (8). A number of point mutations were found to be unable to rescue incorrect localization of the $InsP_3$ receptor in cardiomyocytes (the ankyrin-B mutants) or misassemble of the lateral membranes of epithelia (ankyrin-G mutants) induced by "knockdown" of endogenous ankyrins, but interestingly these mutations do not disrupt the ankyrin/spectrin interaction (8). Strikingly, by mapping the mutations in ankyrin-B to the structure, we found that almost all the mutated residues are located within or in the vicinity of the ZU5^N/UPA interface (Fig. 3*C*). Three of such mutation sites of ankyrin-B, R1105$_{ZU5N}$, D1322$_{UPA}$, and D1339$_{UPA}$, are involved in forming the three charge pairs in the ZU5^N/UPA interface (Fig. 3*A*). A more recent study found that ankyrin-B interacts with dynactin-4 (21). Substitution of D1319$_{UPA}$ with alanine impairs the ankyrin-B/dynactin-4 interaction but does not interfere with the spectrin-binding ability of ankyrin-B (21). D1319$_{UPA}$ forms the buried salt bridge with R1029$_{ZU5N}$ in the ZU5^N/UPA interface (Fig. 3*A*), and the mutation is expected to disrupt the ZU5^N/UPA interaction of ankyrin-B. Like the mutations in ankyrin-B, the mutations in ankyrin-G are also localized in the ZU5^N/UPA interface (Fig. 3*D*). Thus, the structure of the ZZUD tandem, together with these mutagenesis data, reveals that the ZU5^N/UPA interaction formed by the conserved charged residues is critical for the non-spectrin-binding functions of SBD, and that the ZZU tandem acts as a structural as well as a functional supramodule for binding to target proteins other than spectrin (e.g. dynactin-4).

Ankyrin-B ZZU Contains Two Additional Potential Target Binding Sites. To gain clues on possible additional target binding, we mapped the degree of amino acid sequence conservation (based on the sequence alignment shown in Fig. 2) to the surface of the ankyrin-B ZZU structure. We found that the highly conserved residues are clustered into two separated regions on the surface of ZZU (Fig. 4). The first one is on ZU5^N and UPA, mainly composed of highly conserved residues from β1, β2, β4, and the loops connecting β1/β2, β2/β3, and β3/β4 of ZU5^N, as well as the C-terminal part of long β2/β3-loop of UPA (Figs. 2 and 4*A*). Part of this region is involved in the binding to spectrin (Fig. 4*A*), substantiating the conclusion that spectrin binding is an evolutionally conserved property for all ankyrins. However, a large part of this region, including the β2/β3-loop of ZU5^N and the β2/β3-loop of UPA, is not involved in the spectrin binding. The solvent-exposed residues in these two loops are not expected to play a structural

role for ZU5^N or UPA. Thus, this conserved surface crossing both ZU5^N and UPA may interact with still unknown target(s), and such interaction(s) is likely to be a common property of all ankyrins. Interestingly, this conserved surface on UPA is partially blocked by the ZU5^N-bound spectrin (Fig. 4*A*), suggesting that the hypothetical binding protein may regulate spectrin binding to ankyrins or vice versa. The second surface is composed of highly conserved residues from β4′, β7′, the β3′/β4′-loop, and the β6′/β7′-loop of ZU5^C (Fig. 4*B*). Most of these conserved surface residues are positively charged, such as K1157, R1158, R1160, R1193, R1194, K1195, H1197, and K1198 (Figs. 2 and 4*B*). It is highly likely that this large, positively charged surface on ZU5^C may function to bind to negatively charged target protein(s). Although the second region does not involve ZU5^N and UPA, the formation of the ZZU supramodule fixes the orientation of ZU5^C in the ZZU supramodule. Obviously, further work is required to test the structure-based predictions of the two additional potential target binding sites common to all ankyrins.

DD is not sequestered by ZZU in ankyrin-B. In the UNC5b ZU5-UPA-DD structure, ZU5 tightly sequesters DD through hydrophobic interactions and prevents the domain from forming homodimer or from interacting with other death domains (17). Because ankryin-B DD and UNC5b DD are similar in both sequence and structure, ankyrin-B DD was originally predicted to be sequestered by its ZU5 domains too. Unexpectedly, the ankyrin-B ZZUD structure reveals that neither ZU5^N nor ZU5^C binds to DD. Compared to the ZU5/DD interface in UNC5b, the corresponding surface in ankyin-B ZU5^N is covered by a loop connecting α1 and β9 (Fig. 1 *A* and *B* and Fig. S1) and thus is not accessible to DD. Although the corresponding surface of ZU5^C is accessible, the corresponding hydrophobic residues critical for the UNC5b ZU5/DD interaction (17) are lacking in ankyrin-B ZU5^C. Therefore, ankyrin-B ZU5^C does not bind to its DD either. Instead, we observe the direct interaction between UPA and DD in the ankyrin-B ZZUD crystal (Fig. 1*A*). This UPA/DD interaction is mediated by several salt bridges formed by residues that are not conserved in other ankyrins (Fig. 2 and Fig. S2*A*), indicating that the UPA/DD interaction is likely to be an artifact of the crystal packing. To test the above prediction, we inserted the human rhinovirus (HRV) 3C protease cleavage site in the long flexible loop between UPA and DD of ankyrin-B. The insertion of the protease cleavage site does not change the elution volume of ZZUD on an analytical gel filtration column (Fig. S2*B*). Protease 3C cleavage of the insertion mutant produced two fragments corresponding to the ZZU tandem and the isolated DD (Fig. S2*C*), indicating that protease released DD does not associate with ZZU in solution. Additionally, we found that the ZZUD tandem and the ZZU tandem binding to spectrin with the same affinity (Table S2), suggesting that the DD/UPA interaction found in the ZZUD crystal does not exist in solution, as otherwise the spectrin R13-14 would physically crash into DD in the ZZUD/spectrin complex (Fig. S3). Therefore, unlike what is found in UNC5b, ankyrin DD is not sequestered by its ZZU tandem, and the domain is free to interact with its potential targets such as Fas DD (22). It is noted that a number of ankyrin-G and -B splicing variants contain large insertions (>1,000 residues) between SBD and DD (23, 24), which may further separate DD from the ZZU tandem.

The Functional Implications of the Disease-Causing Mutations in ZZUD. A total of eight inherited missense mutations involving seven residues in ankyrin-B ZZUD have been reported in patients with the ankyrin-B syndrome (25–29), and three loss-of-function mutations in ankyrin-R ZZUD were found to cause hereditary spherocytosis (9). Our structure provides insights into the mechanistic bases of the diseases caused by these mutations. The eight ankyrin-B syndrome-causing mutations are T1404I, G1406C, E1425G, R1450W, E1452K, L1503V, V1516I, and V1516D. Four out of the seven mutation sites are located in two disordered loops (T1404 and G1406 in the β2/β3-loop of UPA; E1425 and R1450 in the loop connecting UPA and DD, Fig. 5). The other three mutation sites (E1452, L1503, and V1516) involve residues on the solvent-exposed surface of DD (Fig. 5). Curiously, most of these seven residues are not conserved among the ankyrin family members (Fig. 2), and none of these mutation sites is involved in the binding of ankyrin to spectrin. Our structural and sequence analysis suggest that these eight ankyrin-B syndrome-causing mutations are not likely to cause overall folding alterations of the domains in the ZZUD tandem, but instead these mutations may change ankyrins' binding to nonspectrin targets. We characterized biochemical properties of two loss-of-function mutations (G1406C and E1415G) of ankyrin-B ZZUD. As predicted, the G1406C and E1425G mutants of ankyrin-B ZZUD showed no observable defects in folding or in the binding to spectrin (Fig. S4 and Table S2). We note with interest that the E1425G mutant of ankyrin-B, which causes human cardiac arrhythmia (25, 26), can directly affect the N-terminal ankyrin repeats-mediated binding of Na/K ATPase, Na/Ca exchanger, and InsP$_3$ receptor (30). These findings suggest

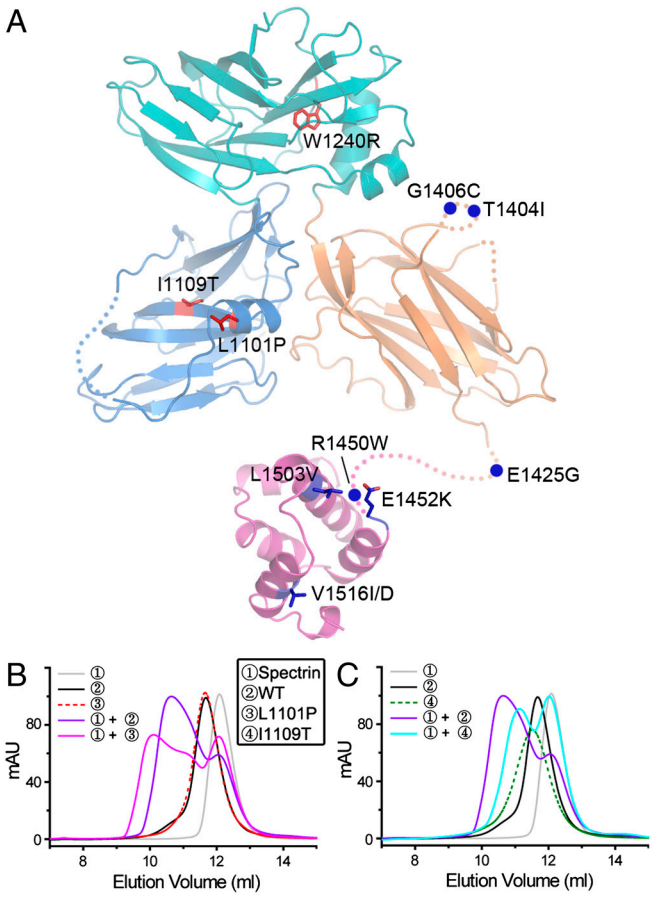

Fig. 5. The disease-causing mutations in the ankyrin ZZUD tandem. (*A*) The disease-causing mutations in ankyrins are mapped onto the structures of the ZZU tandem and DD. The ankyrin-B syndrome mutations and hereditary spherocytosis mutations in ankyrin-R are colored in blue and red, respectively. The disordered loops are indicated by dotted lines. (*B*) Analytical gel filtration chromatography comparing the interactions of the wild-type (WT) ankyrin-B ZZUD and the L1101P mutant with β-spectrin R14-15. The L1101P mutant formed multiple complex peaks with β-spectrin R14-15. (*C*) The interactions of the WT ankyrin-B ZZUD and the I1109T mutant with β-spectrin R14-15. The I1109T mutant/β-spectrin R14-15 complex was eluted at a larger volume compared to the WT ZZUD, indicating that the mutant has a somewhat weaker binding to β-spectrin.

that the ankyrin-B ZZUD tandem is likely to bind to other proteins, thereby to regulate its N-terminal ankyrin repeats-mediated membrane binding. The three disease-causing mutations of ankyrin-R (L1046P, I1054T, and W1185R) involve three highly conserved residues, corresponding to L1101 and I1109 in $ZU5^N$ and W1240 in $ZU5^C$ in ankyrin-B, indicating that these three residues play common roles for all ankyrins. Based on the ankyrin-B ZZUD structure, all these residues, W1240 in particular, are involved in the formation of the hydrophobic cores of either $ZU5^N$ or $ZU5^C$ (Fig. 5 and Fig. S5). The mutations of any one of these three residues are expected to alter the conformation of $ZU5^N$ or $ZU5^C$ and therefore impair the function of ankyrin-R. To test the above hypothesis, we characterized all three mutants of ankyrin-B ZZUD. The W1240R mutant displayed rapid degradation during protein purification, and we were not able to obtain any purified protein for biochemical characterization. Because W1240 forms the folding core of $ZU5^C$ (Fig. S5*B*), and substitution of the bulky tryptophan with positively charged arginine is expected to disrupt the folding and thus the function of the protein. Circular dichroism-based protein stability studies showed that the L1101P or the I1109T substitutions only displayed marginal impact on the overall folding of the ZZUD tandem (Fig. S4). Because L1101 and I1109 are both localized in $ZU5^N$ (Fig. S5*A*), we tested possible impact of each mutation on ZZUD's binding to spectrin. Although the L1101P mutant can still bind to spectrin (Fig. S7), the complex formed is heterogeneous (Fig. 5*B*), indicating that the L1101P mutation can cause misassembly of the ankyrin/spectrin complex. The ZZUD_I1109T mutant showed a weakened spectrin binding (Fig. 5*C*). Therefore, the ZZUD structure provides a mechanistic basis for understanding ankyrin-R mutation-induced spherocytosis in humans. It is noted that the mutation of W1185 in ankyrin-R, which is located in $ZU5^C$ and not involved in spectrin binding, can cause hereditary spherocytosis, further indicating that $ZU5^C$-mediated binding(s) to nonspectrin target is important functional property of ankyrins.

The PIDDosome organization center PIDD also contains two ZU5 domains in its ZZUD tandem (Fig. 1*C*). A structure-based analysis of the PIDD amino acid sequence suggests that the ZZU tandem of PIDD may adopt a similar supramodular conformation to that of ankyrin-B shown in the current study rather than that of UNC5b (Fig. S6). The ankyrin-B ZZUD structure can be used as a valuable template for exploring the molecular basis underlying apoptosis mediated by the PIDD-assembled cell death machinery (31).

In conclusion, we have solved the crystal structure of ankyrin-B ZZUD. The intramolecular interactions of $ZU5^N$/UPA and $ZU5^N$/$ZU5^C$ stabilize the ZZU architecture. The extensive $ZU5^N$/UPA interaction provides a mechanistic explanation for previously identified functional deficient mutations found in ankyrin-B&G. The structure further indicates that the previously coined spectrin-binding domain of ankyrins binds to target proteins in addition to spectrin. Unlike UNC5b ZU5-UPA-DD, ankyrin-B DD is not sequestered by its own ZZU. Finally, the ankyrin-B ZZUD structure provides mechanistic explanations to many disease-causing mutations identified in ankyrins.

Materials and Methods

The ankyrin-B ZZUD protein was expressed in *Escherichia coli* BL21(DE3) and purified by Ni^{2+}-NTA affinity chromatography followed by size-exclusion chromatography. Crystals were obtained by hanging drop vapor diffusion method at 16 °C in 18% w/v PEG3350 and 0.2 M ammonium acetate. An extended method describing protein preparation, crystallization, structure determination, and biochemical assays can be found in *SI Materials and Methods*.

ACKNOWLEDGMENTS. We thank Vann Bennett for providing the ankyrin-B cDNA construct and the BL17U beamline of the Shanghai Synchrotron Radiation Facility for the beamline time. This work was supported by grants from the Research Grants Council of Hong Kong to M.Z. (663808, 664009, 660709, 663610, 663811, HKUST6/CRF/10, and SEG_HKUST06) and to Z.W. (662710). Z.W. is a fellow of the Tin Ka Ping Foundation under IAS of HKUST.

1. Bennett V, Baines AJ (2001) Spectrin and ankyrin-based pathways: Metazoan inventions for integrating cells into tissues. *Physiol Rev* 81:1353–1392.
2. Bennett V, Healy J (2009) Membrane domains based on ankyrin and spectrin associated with cell-cell interactions. *Cold Spring Harb Perspect Biol* 1:a003012.
3. Bennett V, Stenbuck PJ (1979) Identification and partial purification of ankyrin, the high affinity membrane attachment site for human erythrocyte spectrin. *J Biol Chem* 254:2533–2541.
4. Bennett V, Healy J (2008) Organizing the fluid membrane bilayer: Diseases linked to spectrin and ankyrin. *Trends Mol Med* 14:28–36.
5. Zhou D, et al. (1998) AnkyrinG is required for clustering of voltage-gated Na channels at axon initial segments and for normal action potential firing. *J Cell Biol* 143:1295–1304.
6. Hedstrom KL, et al. (2007) Neurofascin assembles a specialized extracellular matrix at the axon initial segment. *J Cell Biol* 178:875–886.
7. Kizhatil K, Bennett V (2004) Lateral membrane biogenesis in human bronchial epithelial cells requires 190-kDa ankyrin-G. *J Biol Chem* 279:16706–16714.
8. Kizhatil K, et al. (2007) Ankyrin-G and beta2-spectrin collaborate in biogenesis of lateral membrane of human bronchial epithelial cells. *J Biol Chem* 282:2029–2037.
9. Gallagher PG (2005) Hematologically important mutations: Ankyrin variants in hereditary spherocytosis. *Blood Cells Mol Dis* 35:345–347.
10. Ferreira MA, et al. (2008) Collaborative genome-wide association analysis supports a role for ANK3 and CACNA1C in bipolar disorder. *Nat Genet* 40:1056–1058.
11. Schulze TG, et al. (2009) Two variants in Ankyrin 3 (ANK3) are independent genetic risk factors for bipolar disorder. *Mol Psychiatry* 14:487–491.
12. Scott LJ, et al. (2009) Genome-wide association and meta-analysis of bipolar disorder in individuals of European ancestry. *Proc Natl Acad Sci USA* 106:7501–7506.
13. Smith EN, et al. (2009) Genome-wide association study of bipolar disorder in European American and African American individuals. *Mol Psychiatry* 14:755–763.
14. Lee MT, et al. (2011) Genome-wide association study of bipolar I disorder in the Han Chinese population. *Mol Psychiatry* 16:548–556.
15. Hashemi SM, Hund TJ, Mohler PJ (2009) Cardiac ankyrins in health and disease. *J Mol Cell Cardiol* 47:203–209.
16. Mohler PJ, Yoon W, Bennett V (2004) Ankyrin-B targets beta2-spectrin to an intracellular compartment in neonatal cardiomyocytes. *J Biol Chem* 279:40185–40193.
17. Wang R, et al. (2009) Autoinhibition of UNC5b revealed by the cytoplasmic domain structure of the receptor. *Mol Cell* 33:692–703.
18. Ipsaro JJ, Mondragon A (2010) Structural basis for spectrin recognition by ankyrin. *Blood* 115:4093–4101.
19. Janssens S, Tinel A, Lippens S, Tschopp J (2005) PIDD mediates NF-kappaB activation in response to DNA damage. *Cell* 123:1079–1092.
20. Ipsaro JJ, Huang L, Gutierrez L, MacDonald RI (2008) Molecular epitopes of the ankyrin-spectrin interaction. *Biochemistry* 47:7452–7464.
21. Ayalon G, et al. (2011) Ankyrin-B interactions with spectrin and dynactin-4 are required for dystrophin-based protection of skeletal muscle from exercise injury. *J Biol Chem* 286:7370–7378.
22. Del Rio M, et al. (2004) The death domain of kidney ankyrin interacts with Fas and promotes Fas-mediated cell death in renal epithelia. *J Am Soc Nephrol* 15:41–51.
23. Chan W, Kordeli E, Bennett V (1993) 440-kD ankyrinB: Structure of the major developmentally regulated domain and selective localization in unmyelinated axons. *J Cell Biol* 123:1463–1473.
24. Kordeli E, Lambert S, Bennett V (1995) AnkyrinG. A new ankyrin gene with neural-specific isoforms localized at the axonal initial segment and node of Ranvier. *J Biol Chem* 270:2352–2359.
25. Mohler PJ, et al. (2003) Ankyrin-B mutation causes type 4 long-QT cardiac arrhythmia and sudden cardiac death. *Nature* 421:634–639.
26. Mohler PJ, et al. (2004) A cardiac arrhythmia syndrome caused by loss of ankyrin-B function. *Proc Natl Acad Sci USA* 101:9137–9142.
27. Mohler PJ, et al. (2007) Defining the cellular phenotype of "ankyrin-B syndrome" variants: Human ANK2 variants associated with clinical phenotypes display a spectrum of activities in cardiomyocytes. *Circulation* 115:432–441.
28. Sherman J, Tester DJ, Ackerman MJ (2005) Targeted mutational analysis of ankyrin-B in 541 consecutive, unrelated patients referred for long QT syndrome genetic testing and 200 healthy subjects. *Heart Rhythm* 2:1218–1223.
29. Mank-Seymour AR, et al. (2006) Association of torsades de pointes with novel and known single nucleotide polymorphisms in long QT syndrome genes. *Am Heart J* 152:1116–1122.
30. Mohler PJ, Davis JQ, Bennett V (2005) Ankyrin-B coordinates the Na/K ATPase, Na/Ca exchanger, and InsP3 receptor in a cardiac T-tubule/SR microdomain. *PLoS Biol* 3:e423.
31. Tinel A, et al. (2007) Autoproteolysis of PIDD marks the bifurcation between pro-death caspase-2 and pro-survival NF-kappaB pathway. *EMBO J* 26:197–208.

Supporting Information

Wang et al. 10.1073/pnas.1200613109

SI Materials and Methods

Protein Expression and purification. The coding sequences of ankyrin-B ZZUD (residues 966–1535) were PCR amplified from the full-length human 220-kDa ankyrin-B, which is a generous gift from Vann Bennett (Duke University) and cloned into the modified pET32a vector. The N-terminal His_6-tagged ZZUD was expressed in *Escherichia coli* BL21(DE3) and purified by Ni^{2+}-NTA affinity chromatography followed by size-exclusion chromatography in the buffer containing 50 mM Tris, 100 mM NaCl, 1 mM EDTA and 1 mM DTT at pH 7.5. The ZZUD mutant used for crystallization with the nine-residue deletion (^{1211}SDVMLNGFG^{1219}) was created using the standard PCR-based mutagenesis method. All point mutations including ankyrin-B ZZUD with residues substituted in the domain interfaces and disease-causing mutations were created using the Quick Change site-directed mutagenesis kit and confirmed by DNA sequencing. The HRV 3C protease-cleavable ZZUD was constructed by replacing the "^{1436}IDMTSEKN^{1443}" fragment of the protein with the protease recognition sequence "LEVLFQGP." The mutant proteins were purified using the procedure identical to that used for the wild-type ZZUD. The coding sequence of human β-spectrin repeats 13–15 (residues 1583–1906) was PCR amplified from a human cDNA library and cloned into the modified pET32a vector. The β-spectrin repeats 13–15 and repeats 14–15 (residues 1686–1906) were purified using the same procedure as that described for the purification of ZZUD.

Analytical Gel Filtration Chromatography. Analytical gel filtration chromatography was carried out on an AKTA FPLC system (GE Healthcare). Proteins were loaded onto a Superose 12 10/300 GL column (GE Healthcare) equilibrated with a buffer containing 50 mM Tris, 100 mM NaCl, 1 mM EDTA and 1 mM DTT at pH 7.5.

Isothermal Titration Calorimetry Assay. Isothermal titration calorimetry (ITC) measurements were carried out on a VP-ITC Microcal calorimeter (Microcal) at 25 °C. All proteins were in 50 mM Tris buffer containing 100 mM NaCl, 1 mM EDTA and 1 mM DTT at pH 7.5. Each titration point was performed by injecting a 10 μL aliquot of β-spectrin R14-15 into various ankyrin protein samples in the cell at a time interval of 120 seconds to ensure that the titration peak returned to the baseline. The titration data were analyzed using the program Origin7.0 and fitted by the one-site binding model.

Analytical Ultracentrifugation. Equilibrium sedimentation experiments were performed using a Beckman proteomelab XL-I ultracentrifuge equipped with a 50Ti rotor. Each equilibrium sedimentation was lasted for 72 h with absorption scanning taken at every 12-h interval. Buffer corrected data were analyzed by Sedfit and Sedphat (http://www.analyticalultracentrifugation.com/default.htm).

Circular Dichroism. CD spectra of WT ankyrin-B ZZUD and its various mutations were measured on a JASCO J-815 CD spectropolarimeter at room temperature using a cell path length of 1 mm. Each spectrum was collected with three scans spanning a spectral window of 200–250 nm. The samples were dissolved in 25 mM Tris buffer containing 50mM NaCl, 0.5 mM EDTA and 0.5 mM DTT at pH 7.5 with the increasing concentrations of urea in the same buffer. The protein concentration used in the CD experiment was 10 μM.

Crystallography. Crystals of ankyrin-B ZZUD were obtained by hanging drop vapour diffusion method at 16 °C. To set up a hanging drop, 1 μL of ZZUD (approximately 12 mg/mL) was mixed with 1 μL of crystallization solution with 18% w/v PEG3350 and 0.2 M ammonium acetate. The diffraction qualities of crystals were improved by adding 5% w/v n-Octyl-β-D-glucoside to the crystallization buffer. The diffraction data were collected at Shanghai Synchrotron Radiation Facility and were processed and scaled using HKL2000 (1).

The initial phase was determined by molecular replacement using the modified structure models of the first ZU5 domain of Ankyrin-R (PDB ID code 3F59), the ZU5 domain of UNC5b (PDB ID code 3G5B), and the death domain of Ankyrin-R (PDB ID code 2YVI). Each asymmetric unit contains one ankyrin-B ZZUD molecule. The phase was improved by density modifications with RESOLVE (2). An incomplete structure model was built manually based on the improved phase. The model was refined in Refmac5 (3) and PHENIX (4). COOT was used for model rebuilding and adjustments (5). In the final stage, an additional TLS refinement was performed in PHENIX. The final refinement statistics are listed in Table S1. All structure figures were prepared by PyMOL (http://www.pymol.org/).

Homology Modeling. The structural model of ankyrin-G ZZUD was built and assessed by SWISS-MODEL (6) using the ankyrin-B ZZUD structure as the template. Due to the high sequence identity (approximately 76%) between the two isoforms, the output model shows high structural similarity (overall rmsd <1.0 Å) with the ankyrin-B ZZUD tandem.

1. Otwinowski Z, Minor W (1997) Processing of X-ray diffraction data collected in oscillation mode. *Methods Enzymol* 276:307–326.
2. Terwilliger TC (2000) Maximum-likelihood density modification. *Acta Crystallogr D Biol Crystallogr* 56:965–972.
3. Murshudov GN, Vagin AA, Dodson EJ (1997) Refinement of macromolecular structures by the maximum-likelihood method. *Acta Crystallogr D Biol Crystallogr* 53:240–255.
4. Adams PD, et al. (2002) PHENIX: Building new software for automated crystallographic structure determination. *Acta Crystallogr D Biol Crystallogr* 58:1948–1954.
5. Emsley P, Cowtan K (2004) Coot: Model-building tools for molecular graphics. *Acta Crystallogr D Biol Crystallogr* 60:2126–2132.
6. Arnold K, Bordoli L, Kopp J, Schwede T (2006) The SWISS-MODEL workspace: A web-based environment for protein structure homology modelling. *Bioinformatics* 22:195–201.

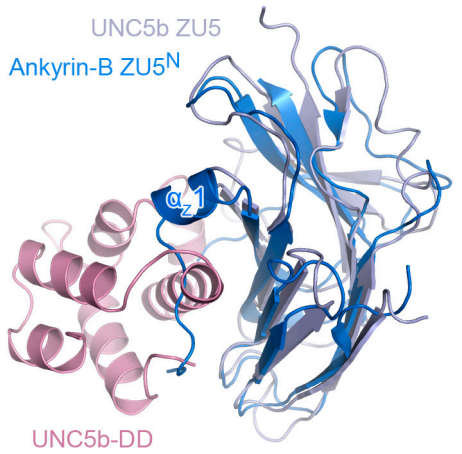

Fig. S1. Superposition of ankyrin-B ZU5^N with UNC5b ZU5 structures showing that the α_Z1 helix together with the following loop prevent the potential interaction between ZU5^N and DD in ankyrin-B.

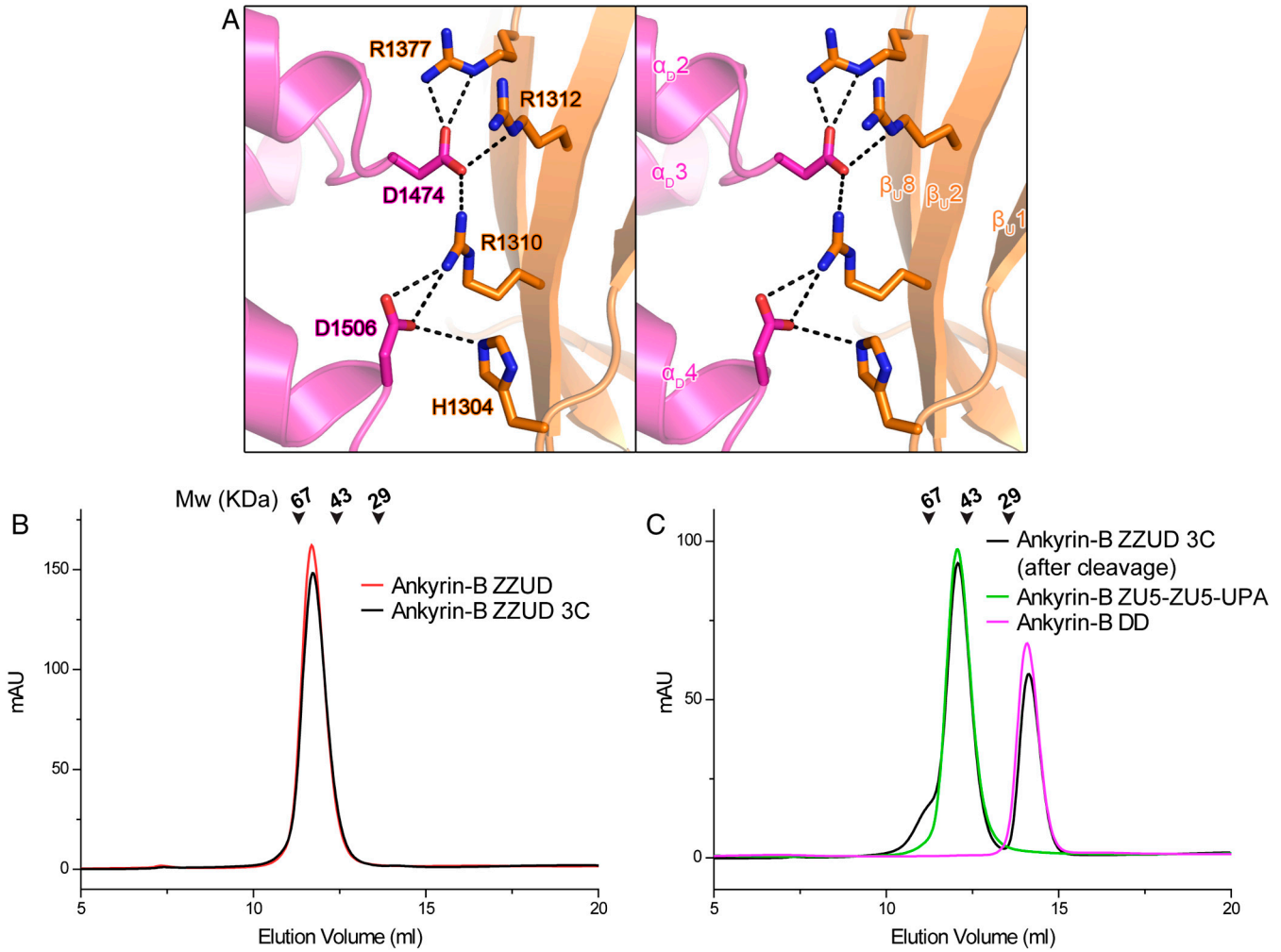

Fig. S2. DD does not associate with the ZZU tandem in ankyrin-B. (*A*) Stereo view showing the UPA/DD interface in the crystal structure of the ankyrin-B ZZUD. The salt bridges are indicated with the dashed lines. (*B*) The engineered insertion of a HRV 3C protease cutting site between UPA and DD did not alter the overall structure of ankyrin-B ZZUD as shown by gel filtration chromatography. (*C*) Gel filtration profile of the HRV 3C protease cleaved ankyrin-B ZZUD 3C mutant showing that DD does not associate with ZZU in solution.

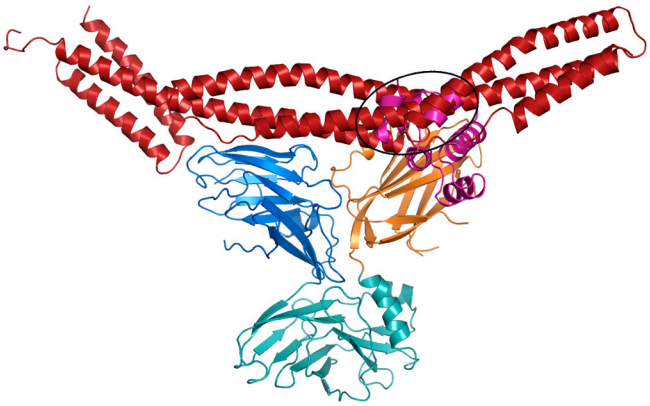

Fig. S3. The ankyrin-B_ZZUD/β-spectrin complex structure model shown in Fig. 4. In this model, the UPA/DD interaction found in the crystal would create a steric hindrance (highlighted by a circle) for the binding of β-spectrin to the ankyrin-B ZZU tandem.

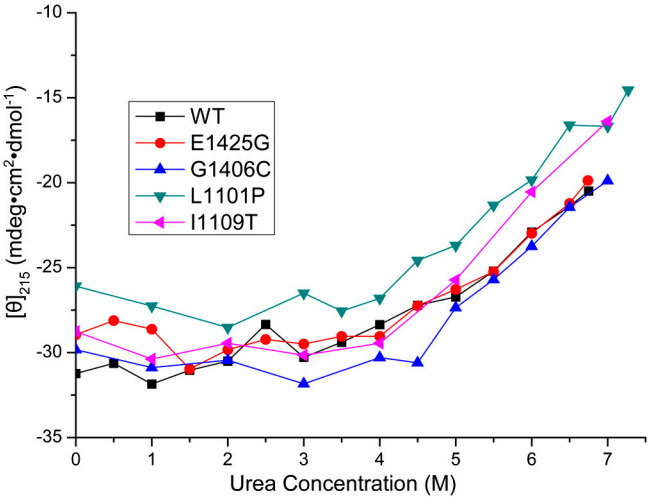

Fig. S4. Urea denaturation-based assay of the stabilities of the WT ankyrin-B ZZUD protein and its four mutants. In this assay, the molar ellipticity values of circular dichroism signals at 215 nm are plotted as a function of urea concentration in the denaturation buffer.

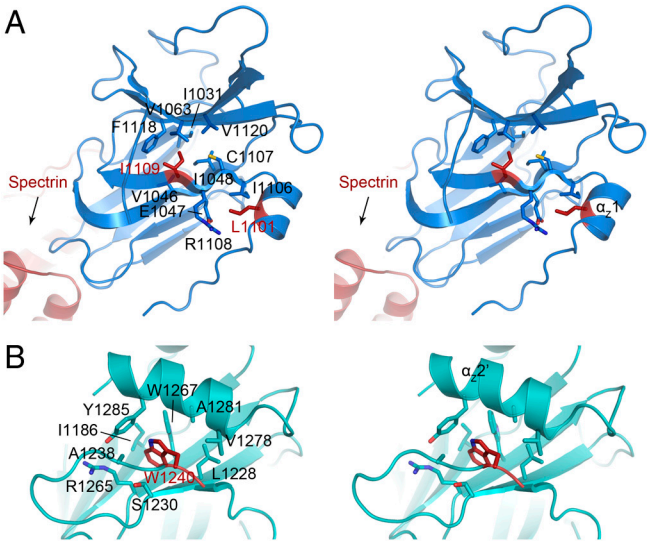

Fig. S5. The combined ribbon and stick representations showing how the three disease-causing mutation residues (I1109, L1101, and W1240) in the ZU5^N (*A*) or ZU5^C (*B*) of the ankyrin-B ZZUD structure.

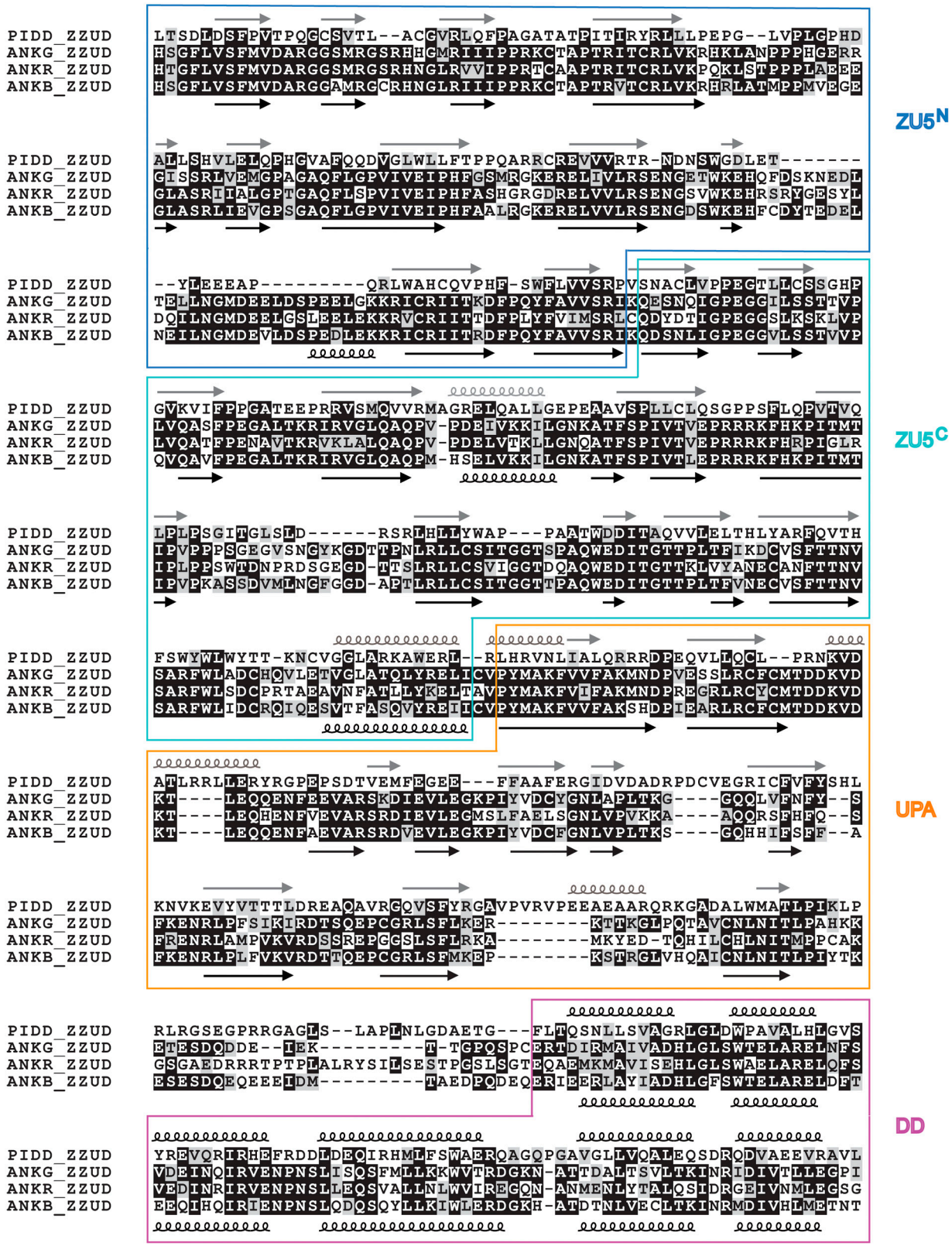

Fig. S6. Amino acid sequence alignment of the ZZUD tandems of human ankyrins and PIDD. The secondary structure elements of PIDD and Ankyrin-B are labeled above and below the alignment, respectively. The secondary structures of the PIDD ZZU tandem are predicted by JPred (http://www.compbio.dundee.ac.uk/www-jpred/) and colored in gray.

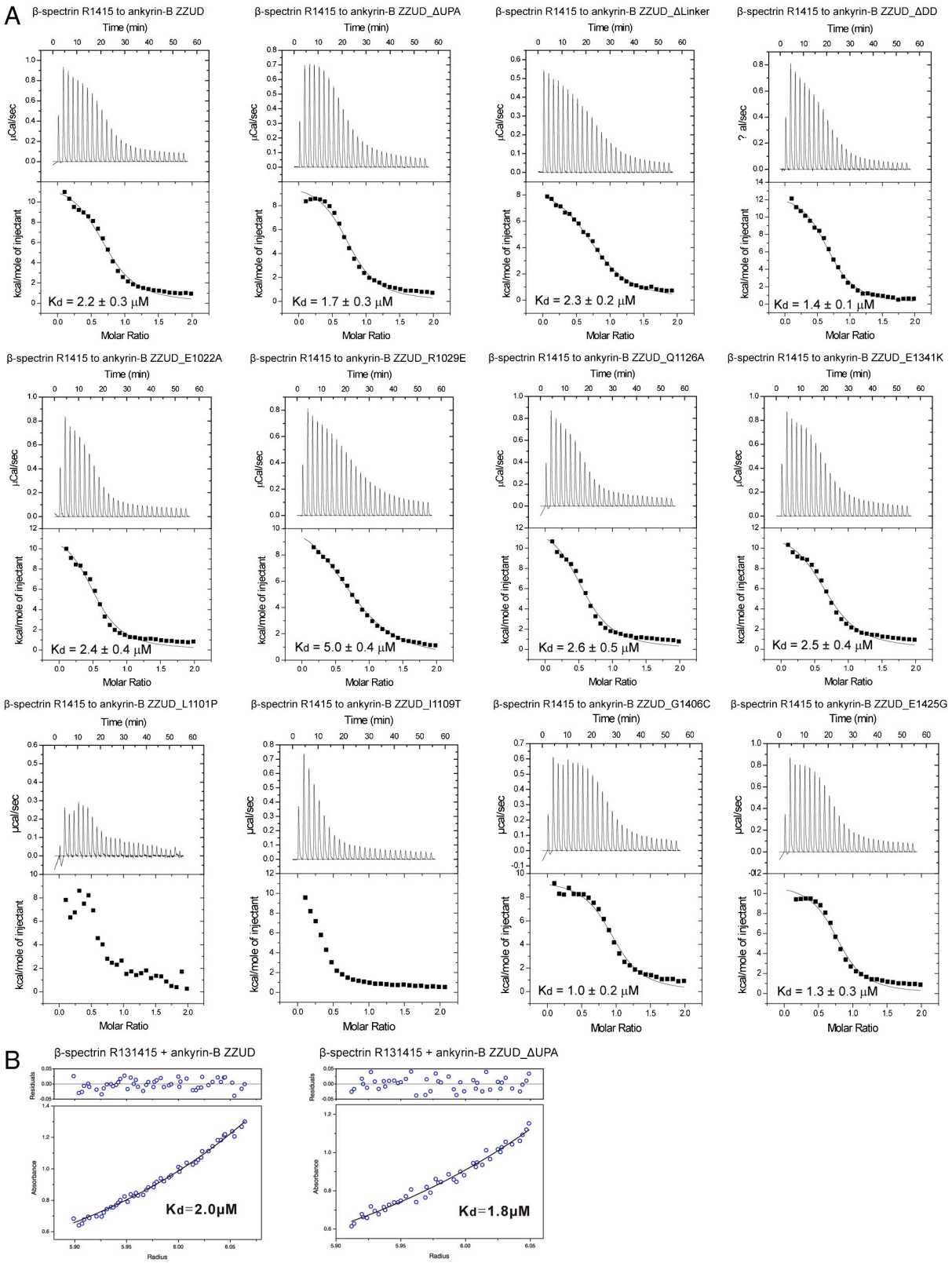

Fig. S7. (*A*) The ITC titration curves for calculating the dissociation constants showing in Table S2. In these binding reactions, the protein concentrations in syringe and in the cell were 0.25 mM and 0.025 mM, respectively. The ITC curves of the L1101P and the I1109T mutants of ankyrin-B ZZUD cannot be reliably fitted, and thus no Kd values are provided in the figure. (*B*) Sedimentation equilibrium analysis of the β-spectrin/ankyrin-B complex. The samples were prepared by mixing β-spectrin R13–15 with ankyrin-B ZZUD or ZZUD_ΔUPA_at 1:1 ratio at a concentration of approximately 10 μM and were centrifuged at 8,700 rpm (ZZUD) or 9,500 rpm (ZZUD_ΔUPA). The curves were fitted using a heterodimer association model and a simulated annealing algorithm.

Table S1. Statistics of data collection and model refinement

Data collection			
Space group		P212121	
Unit cell parameters (Å)		$a = 75.7$, $b = 80.1$, $c = 95.0$	
Resolution range (Å)		50–2.2 (2.24–2.2)	
No. of unique reflections		29,634 (1,458)	
Redundancy		6.8 (7.3)	
I/σ		21.5 (4.3)	
Completeness (%)		99.4 (100.0)	
R_{merge} (%)*		8.5 (48.3)	
Structure refinement			
Resolution (Å)		50–2.2 (2.28–2.2)	
R_{cryst}/R_{free} (%)†	20.8 (25.4) / 24.5 (29.9)	rmsd bonds (Å)/angles (°)	0.005/0.87
No. of reflections		No. of atoms	
working set	26,945	protein atoms	3,989
test set	1,457	water molecules	101
Average B-factor (Å2)		Ramachandran plot regions‡	
main chain	54.7	favored regions (%)	96.6
side chain	60.3	allowed regions (%)	100.0
water	47.1	outliner (%)	0.0

Numbers in parentheses represent the value for the highest resolution shell.

*$R_{merge} = \sum |I_i\text{-}I_m| / \sum I_i$, where I_i is the intensity of the measured reflection and I_m is the mean intensity of all symmetry related reflections.

†$R_{cryst} = \sum ||F_{obs}|\text{-}|F_{calc}|| / \sum |F_{obs}|$, where F_{obs} and F_{calc} are observed and calculated structure factors. $R_{free} = \sum_T ||F_{obs}|\text{-}|F_{calc}|| / \sum_T |F_{obs}|$, where T is a test dataset of about 5% of the total reflections randomly chosen and set aside prior to refinement.

‡Defined by MolProbity (1).

1. Davis IW, et al. (2007) MolProbity: All-atom contacts and structure validation for proteins and nucleic acids. *Nucleic Acids Res* 35:W375–383.

Table S2. Dissociation constants of bindings between various forms of ankyrin-B ZZUD and β-spectrin

	K_d-ITC (μM)*	K_d-AUC (μM)*
ZZUD	2.2 ± 0.3	2.0
ΔUPA	1.7 ± 0.3	1.8
ΔDD	1.4 ± 0.1	n.d.
Δlinker	2.3 ± 0.2	n.d.
E1022A	2.4 ± 0.4	n.d.
R1029E	5.0 ± 0.4	n.d.
Q1126A	2.6 ± 0.5	n.d.
E1341K	2.5 ± 0.4	n.d.
L1101P	n.d.†	n.d.
I1109T	n.d.†	n.d.
G1406C	1.0 ± 0.2	n.d.
E1425G	1.3 ± 0.3	n.d.

*The K_d values are calculated based on the ITC and AUC curves shown in Fig. S7.

†The ITC data cannot be used to fit a reliable K_d value.